Excited-State Electronic Asymmetry of the Special Pair in Photosynthetic Reaction Center Mutants: Absorption and Stark Spectroscopy†

Laura J. Moore, Huilin Zhou, and Steven G. Boxer*

Department of Chemistry, Stanford University, Stanford, California 94305-5080

Received April 19, 1999

ABSTRACT: The electronic absorption line shape and Stark spectrum of the lowest energy Q_y transition of the special pair in bacterial reaction centers contain a wealth of information on mixing with charge transfer states and electronic asymmetry. Both vary greatly in mutants that perturb the chemical composition of the special pair, such as the heterodimer mutants, and in mutants that alter interactions between the special pair and the surrounding reaction center protein, such as those that add or remove hydrogen bonds. The conventional and higher-order Stark spectra of a series of mutants are presented with the aim of developing a systematic description of the electronic structure of the excited state of the special pair that initiates photosynthetic charge separation. The mutants L168HF, M197FH, L131LH and L131LH/M160LH/M197FH are known to have different hydrogen-bonding patterns to the special pair; however, they exhibit Stark effects that are very similar to wild type. By contrast, the addition of a hydrogen bond to the M-side keto carbonyl group of the special pair in M160LH greatly affects both the absorption and Stark spectra. The heterodimer special pairs, L173HL and M202HL, exhibit much larger Stark effects than wild type, with the greatest effect in the M-side mutant. Double mutants that combine the M-side heterodimer and a hydrogen-bond addition to the L-side of the special pair decrease the magnitude of the Stark effect. These results suggest that the electronic asymmetry of the dimer can be perturbed either by the formation of a heterodimer or by adding or deleting a hydrogen bond to a keto carbonyl group. From the pattern observed, it is concluded that the charge transfer state $P_L^+P_M^-$ has a larger influence on the excited state of the dimer in wild type than the $P_L^-P_M^+$charge transfer state. Furthermore, asymmetry can be varied continuously, from extreme cases in which the heterodimer and hydrogen-bond effects work together, to cases in which hydrogen bonding offsets the effects of the heterodimer, to cases in which the homodimer is perturbed by hydrogen bonds. This leads to a unified model for understanding the effects of perturbations on the electronic symmetry of the special pair, and this can be connected with perturbations on the properties of many other systems such as donor−acceptor-substituted polyenes.

Photoexcitation of a strongly interacting pair of bacteriochlorophyll (BChl)[1] molecules called the special pair or P in bacterial photosynthetic reaction centers (RCs) initiates a series of light-driven charge separation reactions. The singlet excited state of P, ^{1}P, transfers an electron within a few picoseconds to H_L, a bacteriopheophytin (BPhe) molecule that is the initial electron acceptor (*1*). As shown in the upper part of Figure 1, there are two similar sets of chromophores related by a local C_2 axis of symmetry that can serve as electron acceptors, yet only the chromophores on the L side (the right side as illustrated, sometimes denoted the *A* branch) participate in the initial charge separation processes. The high level of structural symmetry is also evident within P itself as illustrated in the lower part of Figure 1. Examination of amino acid residues in the immediate vicinity of P reveals one obvious source of environmental asymmetry, the presence of a hydrogen bond from histidine L168 to P_L, one of the bacteriochlorophylls comprising P. As it is generally believed that some combination of symmetry-breaking amino acid differences on the L and M branches of the RC is the origin of unidirectional electron transfer, it is interesting to investigate the electronic asymmetry of the special pair caused by environmental perturbations, and this is the purpose of the present investigation.

Previous data suggest that ^{1}P is not electronically C_2 symmetric; that is, the local symmetry is broken upon photoexcitation. In particular, Stark spectroscopy shows that a substantial separation of charge occurs upon photoexcitation of P, and the change in dipole moment between the ground and excited state, $\Delta\mu$, is substantially larger for P than for a monomeric BChl (*2*). Significantly, the measured angle ζ_A between $\Delta\mu$ and the transition dipole moment of P demonstrates that $\Delta\mu$ is not parallel to the C_2 symmetry axis. This suggests that $\Delta\mu$ for P cannot simply be an equally weighted vector sum of $\Delta\mu$ for each BChl in the dimer, as the resulting $\Delta\mu$ would lie along the C_2 axis (*2*). These spectroscopic observables describe the difference between the ground- and excited-state properties of P at the instant of photoexcitation. Additional changes may occur during the

† This work is supported in part by the NSF Biophysics Program.

* Corresponding author: Phone (650) 723-4482; Fax (650) 723-4817; E-mail Sboxer@leland.stanford.edu.

[1] Abbreviations: BChl, bacteriochlorophyll; BPhe, bacteriopheophytin; CT, charge transfer; ENDOR, electron−nuclear double resonance; EPR, electron paramagnetic resonance; FTIR, Fourier transform infrared; ITO, indium tin oxide; LDAO, lauryldimethylamine *N*-oxide; RC, reaction center.

10.1021/bi990892j CCC: $18.00
Published on Web 08/20/1999

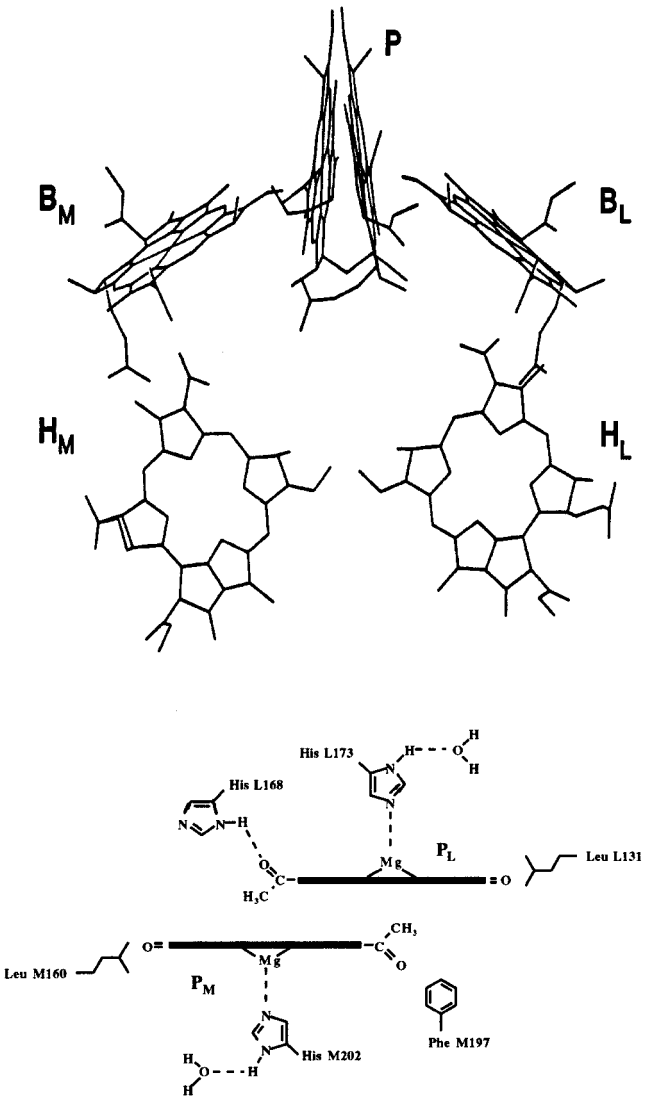

FIGURE 1: Schematic diagram of the chromophore arrangement (upper panel) derived from X-ray structures of reaction centers (*48*) and an enlarged cross-sectional view of the special pair (lower panel) showing amino acids residues in wild type that have been altered by site-directed mutagenesis.

^{1}P lifetime prior to electron transfer, but there are few data on this point. There have been many studies using EPR and ENDOR spectroscopy of P^+, the product of the initial charge separation reaction, that demonstrate that the hole is not equally shared by the two halves of the special pair (*3*, *4*). These measurements are typically made on a long time scale compared to the initial charge separation processes. Additionally, an absorption band has been observed centered at about 2600 cm^{-1} when the special pair is oxidized (*5*), and this has been attributed to the transition between the nondegenerate $P_L^+P_M$ and $P_MP_L^+$ states (*6*). Likewise, the triplet state of P has been shown to possess significant charge-transfer character (*7*, *8*). The relationship among these different observables will be discussed below.

The influence of amino acids in the vicinity of P, shown in the lower part of Figure 1, has been explored in several studies. If either Mg-ligating histidine residue is replaced with Leu, a heterodimer is formed in which one of the BChls is replaced by a bacteriopheophytin (BChl in which the Mg is replaced by two hydrogen atoms) (*9*). The special pairs in these RCs have significantly altered spectroscopic (*10*, *11*) and functional properties (*12*). Mutants have been designed in which the histidine residue (His L168) that is hydrogen-bonded to the peripheral conjugated carbonyl group is removed or in which non-hydrogen-bonding amino acids near to conjugated carbonyl groups of P (residues M160, L131, and M197) are replaced by histidine residues that are capable of forming hydrogen bonds (*13*−*16*). The presence or absence of these hydrogen bonds leads to changes in the carbonyl stretch frequency detected by FTIR (*17*) and FT Raman spectroscopies (*18*−*20*). These hydrogen-bond mutants exhibit large and systematic variations in the oxidation potential of the special pair (*16*, *20*).

Interesting changes are also observed in the electronic absorption spectra of these mutants, but no systematic study has been presented. There has been considerable speculation on the role of the internal charge transfer (CT) states, e.g., $P_L^+P_M^-$ and $P_L^-P_M^+$, and their influence on the properties of the dimer electronic transitions (*21*−*25*). In a simple one-electron picture, such states are likely to be close in energy to the pure exciton states of the dimer. The relative energy, reorganization energy, and electronic coupling of these intradimer CT states with the exciton states should have a substantial effect on the electronic properties of ^{1}P. Furthermore, changes in the hydrogen bonding or formation of a heterodimer should alter the energies of these internal CT states, as addition of a hydrogen bond or removal of the Mg from one side of the dimer should make that side harder to oxidize and easier to reduce.

In a recent paper (*26*), we modeled the line shape of the Q_y electronic absorption band for the heterodimer mutant M202HL ($BChl_LBPhe_M$) in *Rhodobacter sphaeroides* using a charge resonance theory. This model consists of three states: the ground state, a pure molecular exciton state, and a vibronically broadened CT state. Two parameters govern the observed absorption line shape: the relative coupling strength R, which is the ratio of the electronic coupling strength to the vibronic bandwidth of the CT state (treated as a Gaussian for simplicity), and the relative energy shift δ, which is given by the location of the exciton state within the vibronic continuum of the CT state. It was shown that the unusual absorption spectrum of the heterodimer special pair could be modeled by using an intermediate coupling strength ($R \sim 0.33$). By examining the effects of the selective addition or deletion of hydrogen bonds to peripheral conjugated carbonyl groups of the heterodimer, it could be demonstrated that the $BChl_L^+BPhe_M^-$ intradimer CT state is closer in energy to the exciton state than the $BChl_L^-BPhe_M^+$ CT state (the latter is expected to be substantially higher in energy since BPhe is more difficult to oxidize than BChl *in vitro* (*27*); the analysis in ref *26* gives the absolute placement of the energies of these states).

In this paper, we address the broader question of whether the native homodimer and hydrogen-bond mutants of the homodimer can be understood within the same qualitative framework as the M202HL heterodimer. For the homodimer special pair in wild-type RCs, it is likely that the energies of $P_L^+P_M^-$ and $P_L^-P_M^+$ are much closer than in the heterodimers, so a correct model must consider interactions with both these CT states. This remains to be developed, and the data presented should serve as an experimental guide for further theoretical studies. Conceptually, one expects a

continuous evolution from the wild-type homodimer in a relatively more symmetric environment to a homodimer in a more asymmetric environment to the extreme case of asymmetry of the heterodimer. Conversely, the extreme asymmetry introduced into the heterodimer mutants by converting a BChl to BPhe can be made more symmetric to some extent by environmental changes such as compensating hydrogen bonds. Furthermore, the overall direction of the electronic asymmetry can be altered as it is imposed locally on one side or the other, either by formation of the $BChl_L$-$BPhe_M$ heterodimer (M202HL) or the reverse $BChl_MBPhe_L$ heterodimer (L173HL) and/or by asymmetric introduction or deletion of hydrogen bonds to conjugated carbonyl groups. As described below, this viewpoint makes a close connection with descriptions of donor−acceptor-substituted polyenes whose electronic properties have been extensively studied (see, e.g., ref *41* for parallel investigations). This places the systematic analysis of the special pair in the RC into a much larger context.

MATERIALS AND METHODS

All mutant RC strains except for L168HG and L173HL were kindly provided by Professors JoAnn Williams, Jim Allen, and Neal Woodbury (*13*, *15*, *16*). The L168HG mutant was prepared as described previously (*28*). The L173HL mutant was engineered with a poly(histidine) tag at the N-terminal end of the M subunit; this poly(histidine) tag has been shown to have no effect on the properties of the RC but greatly facilitates RC isolation (*29*). RCs were obtained from *Rb. sphaeroides* cells grown under semiaerobic conditions in the dark (*30*).

Stark and absorption spectra of the Q_y bands were obtained at 77 K for RCs in 50/50 (v/v) glycerol/buffer (10 mM Tris, pH 8, and 0.05% LDAO) glasses with a typical OD of 0.35 at 800 nm. The Stark sample cell was constructed from two glass slides coated with 1700 Å of indium tin oxide (ITO) and separated by a 25 μm Kapton spacer. The sample was immersed in liquid nitrogen in a dewar with strain-free quartz windows. The thickness of the sample was measured with a micrometer or calculated from the interference fringes present in the normal incidence absorption spectra. The values obtained from the two methods were in agreement to 1.0 μm. Applied field strengths ranged from 0.6 to 0.8 MV/cm.

Stark spectra were obtained by use of lockin detection as described previously (*31*, *32*). A digitally synthesized low-distortion sine wave from the lockin amplifier was amplified, producing an AC voltage across the sample. The lockin amplifier was set to detect an even harmonic (2ω or 4ω) of the field modulation frequency ω, and the corresponding Stark spectra are denoted 2ω or 4ω. The absorption was probed with horizontally polarized light, and a Si photodiode was used to detect ΔI and I. Spectra were acquired at normal incidence where the angle χ between the electric field vector of the probe light and the applied field direction is 90° and at least one other angle (typically $\chi \sim 50°$). The value of χ was determined from the absorption spectrum at each angle by taking the ratio of the absorption at the angle relative to that at normal incidence and computing the angle from the difference in path lengths. The amplitudes of Stark spectra at angles other than normal incidence were corrected for the change in the absorption due to the change in path length.

For frozen, isotropic samples, the conventional or 2ω Stark spectrum can be described as the sum of derivatives of the absorption spectrum (*33*, *34*):

$$\Delta A(\bar{\nu},F^2,2\omega) = (fF_{ext})^2 \times \left\{ A_\chi A(\bar{\nu}) + \frac{B_x}{15hc}\frac{\bar{\nu}\,\mathrm{d}\left[\frac{A(\bar{\nu})}{\bar{\nu}}\right]}{\mathrm{d}\bar{\nu}} + \frac{C_\chi}{30h^2c^2}\frac{\bar{\nu}\mathrm{d}^2\left[\frac{A(\bar{\nu})}{\bar{\nu}}\right]}{\mathrm{d}\bar{\nu}^2} \right\} \quad (1)$$

where F_{ext} is the external applied field, f is the local field correction,[2] h is Planck's constant, and c is the speed of light. The coefficients $A\chi$, B_χ, and C_χ are associated with the molecular properties of the system. A_χ is related to the change in the transition moment upon application of an applied field, B_χ is associated with the change in polarizability $\Delta\alpha$ between the ground and excited states, and C_χ is given by

$$C_\chi = \Delta\mu^2[5 + (3\cos^2\chi - 1)(3\cos^2\zeta_A - 1)] \quad (2)$$

C_χ depends only on $\Delta\mu$ and ζ_A, the angle between $\Delta\mu$ and the transition moment direction. For our purposes, only the magnitude of the second-derivative component in a Stark spectrum will be considered, and this is only related to $\Delta\mu$ (*35*). ζ_A was determined from the ratio of the Stark spectra taken at different experimental angles χ.

If $\Delta\mu$ dominates the Stark effect, the same $\Delta\mu$ can be determined from the 4ω Stark spectrum (*36*). In this case, the numerical second derivative of the experimental 2ω Stark spectrum should share the same line shape as the experimental 4ω Stark spectrum, and their amplitude ratio can be used to determine $\Delta\mu$ directly:

$$\frac{\Delta A(\bar{\nu},4\omega)}{\bar{\nu}\,\mathrm{d}^2\left[\frac{\Delta A(\bar{\nu},2\omega)}{\bar{\nu}}\right]/\mathrm{d}\bar{\nu}^2} = \frac{\Delta\mu^2F^2[7 + 2(3\cos^2\chi - 1)(3\cos^2\zeta_A - 1)]}{28h^2c^2[5 + (3\cos^2\chi - 1)(3\cos^2\zeta_A - 1)]} \quad (3)$$

where $\bar{\nu}\,\mathrm{d}^2[\Delta A(\bar{\nu},2\omega)/\bar{\nu}]/\mathrm{d}\bar{\nu}^2$ is the ν-weighted second derivative of the 2ω Stark spectrum obtained by numerical differentiation.

To obtain derivatives of the absorption spectra at 77 K it was necessary to acquire absorption spectra without interference fringes and with a high signal-to-noise ratio. Therefore, absorption spectra were taken at an angle other than normal incidence with a double-beam Perkin-Elmer Lambda 12 spectrometer. The absorption spectrum amplitude was then matched to the one taken with the Stark apparatus. The

[2] The local electric field at the molecule is equal to the external (applied) field F_{ext} multiplied by the local field correction f. The local field correction is related to the dielectric constant of the medium and the shape of the cavity, which should be approximately the same for all the mutants. For simplicity, subsequent references to the field will use the notation F and the values obtained for the difference dipole will be reported as debyes/f.

Table 1: Absorption and Stark Band Positions and Absorption Full Widths at Half-Maximum for the Special Pair Q_y Transitions in Reaction Center Mutants[a]

reaction center	absorption maximum	absorption FWHM	minimum of 2ω Stark spectrum	maximum of 4ω Stark spectrum
wild type	11220	570	11250	11310
L131LH	11190	730	11190	~11100
M160LH	11160	~1000	10930	10900
L173HL	11380	>1000	11180	11150
M202HL	11000	nd	10700	10670
	11800			
M202HL/L131LH	11160	>1000	11000	10970
M202HL/M160LH	10500	nd	10300	10260
	11500		11500	11500
L168HF	11470	670	11450	11500
L168HG	11360	730	11190	11190
L168HF /M197FH	11740	660	11740	11810
M197FH	11260	550	11200	11150
L131LH/M160LH/M197FH	11270	630	11220	11170

[a] Measurements were made in 50% glycerol at 77 K. All values are given in reciprocal centimeters.

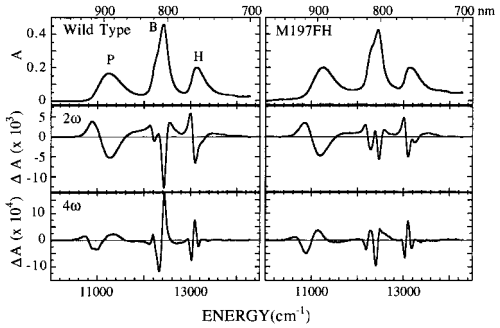

FIGURE 2: Absorption (top), 2ω (middle), and 4ω (bottom) Stark spectra of *Rb. sphaeroides* RCs for wild type (left) and the M197FH mutant (right) in the Q_y region at 77 K. The bands associated with the special pair (P), the bacteriochlorophyll monomers (B), and the bacteriopheophytins (H) are labeled (cf. Figure 1). The absorption spectra were scaled to an optical density of 0.2 at 760 nm, and the Stark spectra were normalized to an applied field of 1.0 MV/cm to facilitate comparison in this and all subsequent figures.

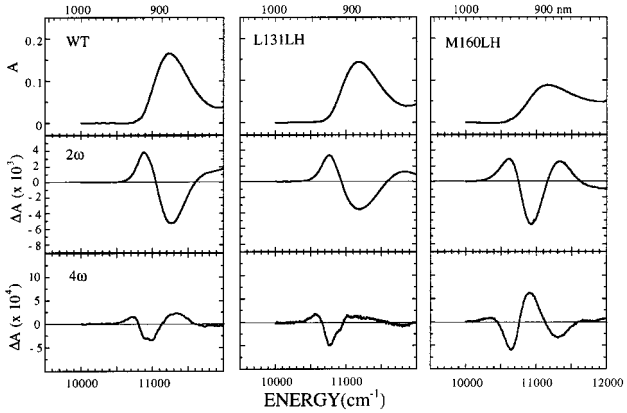

FIGURE 3: Absorption (top), 2ω (middle), and 4ω (bottom) Stark spectra of the dimer band of WT (left), L131LH mutant (center), and M160LH mutant (right). The mutations add a hydrogen bond to the ring E keto carbonyl on opposite ends of the dimer (cf. Figure 1).

monochromator on the Stark apparatus and the spectrophotometer had approximately the same resolution (1.7 versus 2 nm).

RESULTS

All spectra presented in the figures were obtained with $\chi = 90°$. The applied electric field strengths have been scaled to a field strength of 1.0 MV/cm, and the absorption spectra were normalized to an OD of 0.2 at 760 nm (see below) to facilitate comparisons. The 2ω Stark spectra depend on F^2 and the 4ω Stark spectra depend on F^4. We begin by describing the results qualitatively, including trends associated with different classes of mutation. This is followed by a more quantitative analysis.

Addition of a Hydrogen Bond to the P_M Acetyl Carbonyl. The absorption, 2ω, and 4ω Stark spectra of the Q_y bands at 77 K for wild type and the M197FH mutant are presented in Figure 2. The absorption of the H band due to the two BPhes can be used for normalization as this band is relatively unchanged by the mutations near the special pair. In all mutants examined, the second derivative of the H-band absorption spectrum matches the line shape of its 2ω Stark spectrum very well. Furthermore, the second derivative of its 2ω Stark spectrum matches the line shape of the 4ω Stark spectrum; thus, as discussed in the Materials and Methods section above and in detail elsewhere (*36*), the H-band Stark spectrum is dominated by $\Delta\mu$. The values of $\Delta\mu$ obtained for the H bands in these mutants fall within a small range from 3.5 to 3.8 D/*f*. As has been shown by Zhou and Boxer (*37*), the higher-order Stark spectrum in the B band region contains an interesting new resonance Stark effect and therefore cannot be used for standardization.

The position and bandwidth of the dimer absorption band in the M197FH mutant are comparable to those of wild type. The position of the minimum in the 2ω Stark spectrum deviates only slightly from the maximum of the absorption band (Table 1), which is also a characteristic of wild type. This suggests that $\Delta\mu$ dominates the Stark effect for M197FH and wild type. Interestingly, the M197FH mutation causes a large variation in the redox potential of the dimer (*16*), despite their nearly identical absorption and Stark spectra.

Mutations That Add a Hydrogen Bond to Keto Carbonyl Groups. The absorption and Stark spectra of the P band for homodimer mutants in which a hydrogen bond has been added to a keto carbonyl at either end of the special pair (see lower part of Figure 1) are compared with WT in Figure 3. The L-side mutant (L131LH, center panel) is similar to wild type (left panel) in both the line shape of the absorption band and the magnitude of the Stark effect. In contrast, the M-side mutant (M160LH, right panel) exhibits a much

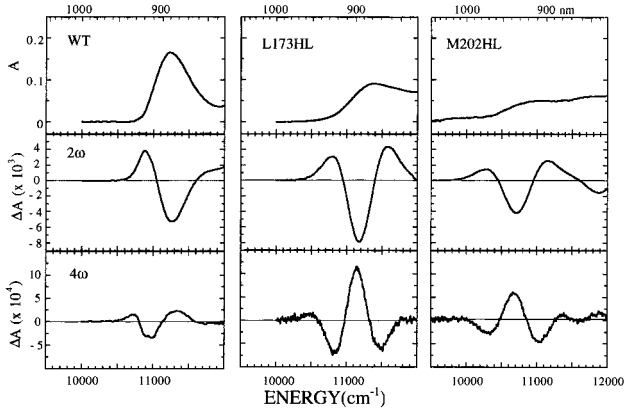

FIGURE 4: Absorption (top), 2ω (middle), and 4ω (bottom) Stark spectra of the dimer band of WT (left), the L173HL mutant (L-side heterodimer, center), and the M202HL mutant (M-side heterodimer, right).

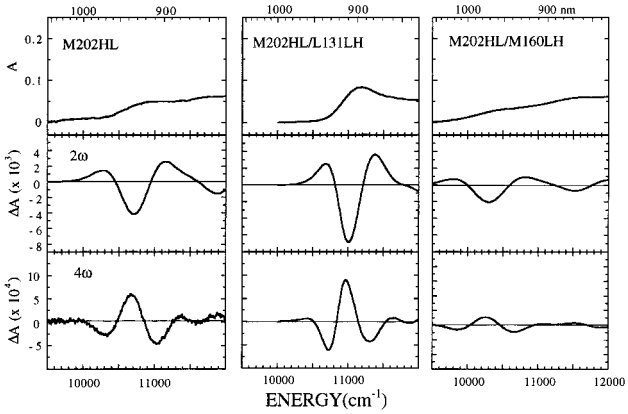

FIGURE 5: Absorption (top), 2ω (middle), and 4ω (bottom) Stark spectra of the dimer band of the M202HL mutant (M-side heterodimer, left), the M202HL/L131LH double mutant (center), and the M202HL/M160LH double mutant (right).

broader absorption line shape, and its Stark spectrum has a larger amplitude and very different line shape than that of the P band in wild type (see Table 1). In the L131LH mutant, the minimum of the 2ω Stark spectrum matches the absorption band maximum. However, for the M160LH mutant, the minimum of the 2ω Stark spectrum is shifted substantially to lower energy by about 230 cm^{-1} compared to the maximum of the absorption band. Qualitatively, two conclusions can be drawn. First, addition of a hydrogen bond to the M-side chromophore of the dimer has a larger effect on the absorption and Stark spectra than the addition of a hydrogen bond to the L-side chromophore. Second, the effect of adding a hydrogen bond to the M-side keto carbonyl group of the special pair produces a larger perturbation on its absorption and Stark spectra than adding a hydrogen bond to the M-side acetyl group.

Heterodimer Mutations. The spectra of the dimer band for the L-side heterodimer (L173HL, the reverse heterodimer) and the M-side heterodimer (M202HL) mutants are compared with wild type in Figure 4. Both heterodimers have spectra that differ significantly from that of wild type. The L173HL mutant (center panel) has a broader absorption band than wild type, while the M202HL mutant (right panel) has a much broader, extended dimer absorption band with two poorly resolved absorption maxima (*10*). The line shapes of the 2ω and 4ω Stark spectra for both heterodimer mutants are very different from that of wild type, and the magnitude of the Stark effect in both mutants is substantially larger than that of wild type. In the L173HL mutant, the minimum of the 2ω Stark spectrum is shifted substantially to lower energy by about 200 cm^{-1} from the maximum of the absorption band. Likewise, the minimum of the 2ω Stark spectrum of the lower-energy feature in the M202HL spectrum is shifted by about 300 cm^{-1} to lower energy from the maximum of the corresponding absorption feature. Interestingly, the absorption and Stark characteristics of the L173HL mutant are similar to those of the homodimer band of M160LH (right panel, Figure 3). Qualitatively it is evident that formation of the M-side heterodimer is a more severe perturbation to the absorption and Stark spectra than formation of the L-side heterodimer.

Heterodimer/Hydrogen-Bond Mutants. The data for two M-side heterodimer/hydrogen-bond double mutants are compared to the M-side heterodimer mutant in Figure 5. Addition of a hydrogen bond to the conjugated carbonyl groups at opposite ends of the dimer (see lower part of Figure 1) produces rather different effects on the heterodimer band. In the M202HL/M160LH mutant, the absorption spectrum of the dimer becomes even broader than that in M202HL. Interestingly, the higher-energy feature around 860 nm is more intense than the lower energy feature around 940 nm in the M202HL/M160LH mutant, whereas the two features have comparable intensities in the M-side heterodimer (*10*). In M202HL/L131LH, where a hydrogen bond is added to the L-side of the dimer (Figure 5, center panel), the dimer absorption band is narrower than that in M202HL, though it is still broader than in WT. In contrast to M202HL/M160LH, the lower energy side of the dimer absorption in M202HL/L131LH contains a prominent absorption peak and no higher-energy absorption feature is discernible from the absorption spectrum. For the Stark spectra, the minimum of the 2ω Stark spectrum of M202HL/L131LH mutant is shifted about 160 cm^{-1} to lower energy than the maximum of the absorption spectrum, while the minimum of the Stark spectrum for the low-energy feature of the M202HL/M160LH double mutant is shifted about 200 cm^{-1} to lower energy compared to the maximum of the absorption. Overall, the M160LH mutation on the M-side of heterodimer M202HL causes the dimer absorption band to become even broader than that of M202HL, while the L131LH mutation on the L-side of heterodimer M202HL reverses the trend and causes the dimer absorption band to be narrower and more similar to WT. Furthermore, the absorption and Stark data of the M202HL/L131LH mutant are strikingly similar to the M-side hydrogen-bond mutant M160LH (right panel, Figure 3) and the L-side (reverse) heterodimer mutant (center panel, Figure 4). The origin of these similarities despite seemingly diverse perturbations will be discussed further below.

Mutations That Remove the Hydrogen Bond from the Acetyl Carbonyl Groups. The spectra for the L168 mutants in which His has been replaced by Phe or Gly are compared with WT in Figure 6. These mutations remove the hydrogen bond between the protein and the acetyl carbonyl group of P_L (see lower part of Figure 1). The P band in both mutants is shifted to higher energy compared to wild type, as has been reported previously for the L168HF mutant (*15*); the

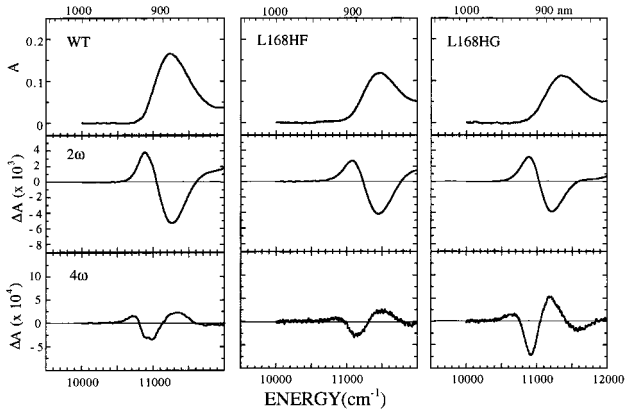

FIGURE 6: Absorption (top), 2ω (middle), and 4ω (bottom) Stark spectra of wild type (left), the L168HF mutant (middle), and the L168HG mutant (right).

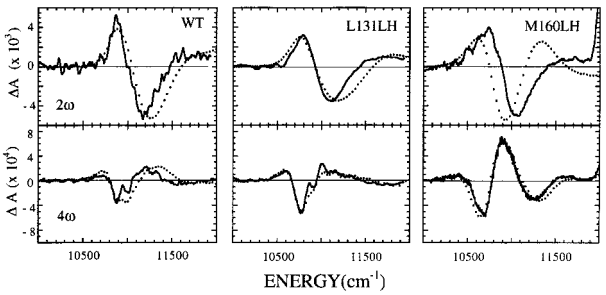

FIGURE 7: Comparison of the 2ω Stark spectra (···) with the ν-weighted second derivative of the absorption (—) (top) and of 4ω Stark spectra (···) with the ν-weighted second derivative 2ω Stark spectrum (—) (bottom) for wild type (left), the L131LH mutant (center), and M160LH mutant (right). The derivatives are multiplied by the following factors to give approximately the same magnitude as the data: wild-type absorption derivative (1200), 2ω Stark derivative (750); L131LH absorption derivative (1400), 2ω Stark derivative (1350); M160LH absorption derivative (4200), 2ω Stark derivative (2200).

bandwidths are only slightly greater than in wild type (Table 1). Although the absorption spectra are similar to each other, there are differences in the shape, position, and magnitude of the Stark spectra. For example, the minimum of the 2ω Stark spectrum for the L168HG mutant is shifted by 170 cm^{-1} to lower energy compared to the maximum of the absorption band, while the minimum of the 2ω Stark spectrum for the L168HF mutant is only slightly shifted ($\sim$20 cm^{-1}) from the maximum of the absorption. Likewise, it is apparent from the 4ω Stark spectrum that the magnitude of the Stark effect is larger in the L168HG mutant.

Multiple Hydrogen-Bond Mutations. Data have also been obtained for the L168HF/M197FH and L131LH/M160LH/M197FH mutants (not shown). The P band of the L168HF/M197FH mutant is shifted 500 cm^{-1} to higher energy compared to that of wild type. Although the band positions of the absorption and Stark spectra appear to be aligned in this double mutant, this evaluation is complicated by overlap of the dimer band with the B band. The Stark and absorption spectra of the L131LH/M160LH/M197FH mutant are essentially identical to those of the single mutant M197FH, and therefore are similar to those of wild type. Since this triple mutant has characteristics of M197FH and not M160LH, it appears that the addition of a hydrogen bond to the L-side keto carbonyl group compensates for the effect of adding a hydrogen bond to the M-side keto carbonyl group.

In summary, two characteristic observations regarding absorption and Stark spectra can be used as a qualitative guide in classifying the independent and combined effects of hydrogen-bond and heterodimer mutations. The width and position of the absorption band compared to that of wild type is the first characteristic used for classification. The magnitude of the Stark effect and position of the minimum of the Stark effect compared to the absorption spectrum maximum is used to further categorize these mutants. The special pair in WT and heterodimer in M202HL can be viewed as two limiting cases. Hydrogen-bond addition to the M-side keto carbonyl group (M160LH) results in a broader P band with a larger Stark effect than in WT. In contrast, hydrogen-bond addition to the symmetry-related L-side keto carbonyl group (L131LH) as well as to the M-side acetyl group (M197FH) appears to have little effect on the Stark or absorption spectra. BChl-to-BPhe modification of the M-side (M202HL) causes the dimer band to be much broader than the corresponding mutation on the L-side (L173HL). Addition of a hydrogen bond to the M-side heterodimer in M202HL/M160LH further broadens the dimer absorption, while addition of hydrogen bond to the L-side in M202HL/L131LH reverses the trend and the dimer absorption band becomes narrower than that in M202HL but still much broader than in WT. Interestingly, the dimer absorption and Stark spectra for M202HL/L131LH and M160LH are very similar despite the fact that the dimer is a heterodimer in the first case but a homodimer in the second. This indicates that the effects of adding a hydrogen bond to the keto carbonyl and BChl-to-BPhe modification on absorption spectra and Stark effects may share a common physical origin, though differing in the effectiveness or strength of the perturbation. Mutants in which the hydrogen bond is removed from the acetyl carbonyl group (L168 mutants) belong to an entirely different category since their absorption spectra are blue-shifted compared to wild type, while the magnitude and shift of the Stark spectra may or may not be similar to wild type.

Quantitative Analysis of Stark Effects. Figure 7 (top panels) shows a comparison of the line shape of the second derivative of the absorption spectra with the 2ω Stark spectra for the three homodimers. This comparison is important because it is the basis on which $\Delta\mu$ is obtained by the type of analysis originally developed by Liptay (*33*). The wild-type 2ω Stark spectrum line shape (Figure 7, left panel) is similar to the second derivative of the absorption spectrum. This agreement of the line shapes suggests that $\Delta\mu$ is the dominant contributor to the Stark spectrum (*35*). In the L131LH mutant (upper middle panel), the second derivative of the absorption is also similar to the 2ω Stark spectrum, again suggesting that $\Delta\mu$ dominates the Stark spectrum. Other reaction centers that fit into this line shape category include L168HF, M197FH, L131LH/M160LH/M197FH, and M197FH/L168HF mutants. In all these mutants, the line shapes of the second derivative of the absorption and the 2ω Stark spectra match well enough so that $|\Delta\mu|$ can be calculated by using eq 2. The calculated difference dipoles range (Table 2) from 5.9 to 7.0 D, all similar to wild type (5.5 D).

In the M160LH mutant (Figure 7, upper right panel), the Stark spectrum is shifted by 200 cm^{-1} to lower energy from

Table 2: Difference Dipole Moments, $|\Delta\mu|$, and Angles ζ_a between $\Delta\mu$ and the Transition Dipole Moment Extracted from the Stark Data

reaction center	$\lvert\Delta\mu\rvert(2\omega)^a$ (D/*f*)	ratio[b]	$\lvert\Delta\mu\rvert(4\omega)^c$ (D/*f*)	$\zeta_a^\circ\ (2\omega)^d$	$\zeta_a^\circ\ (4\omega)^e$
wild type	5.5 ± 0.5	800 ± 80	7.5 ± 1.0	44 ± 2	44 ± 2
L131LH	5.9 ± 0.5	1440 ± 90	10.1 ± 0.3	40 ± 3	34 ± 3
L168HF	6.9 ± 0.3	1410 ± 130	10 ± 0.5	35 ± 2	34 ± 2
L168HG		2270 ± 180		39 ± 2	37 ± 3
M160LH		2380 ± 180		40 ± 2	34 ± 3
M197FH	6.0 ± 0.5	1350 ± 150	9.8 ± 0.5	46 ± 3	47 ± 3
L168HF/M197FH	7.0 ± 0.5	1410 ± 130	10.0 ± 0.5	32 ± 3	31 ± 2
L131LH/M160LH/M197FH	6.7 ± 0.3	1550 ± 150	10.5 ± 0.5	47 ± 2	45 ± 2
L173HL		2880 ± 200		32 ± 2	32 ± 2
M202HL		4560 ± 500		36 ± 2	36 ± 2
M202HL/L131LH		2380 ± 300		39 ± 2	38 ± 2
M202HL/M160LH		5080 ± 500		30 ± 2	32 ± 2

[a] $|\Delta\mu|$ was obtained from the ratio of the second derivative of the absorption and the 2ω Stark spectrum (eqs 1 and 2). For those mutants for which the Stark line shape deviates significantly from the shape of the second derivative or for which a second derivative of the absorption could not be obtained, $|\Delta\mu|$ was not obtained by this method. [b] Ratio of 4ω Stark to the second derivative of 2ω Stark at $F = 1.0$ MV/cm and $\chi = 54.7°$ (to eliminate angle dependence). [c] $|\Delta\mu|$ was obtained from the ratio of the second derivative of the 2ω Stark spectrum and the 4ω Stark spectrum (eq 3). [d] Obtained from the ratio of the 2ω Stark signal at different experimental angles χ. [e] Obtained from the ratio of the 4ω Stark signal at different experimental angles χ.

the minimum of the second derivative of the absorption, and the shape of the 2ω Stark spectrum deviates significantly from that of the second derivative of the absorption spectrum. Other mutants that belong in this category include L173HL, L168HG, and M202HL/L131LH. In all these mutants, the Liptay model of the Stark spectrum based on the derivatives of the absorption spectrum does not work, since even if the first and zeroth derivatives of the absorption spectrum are used in the model, the large shift in the Stark spectra cannot be explained. Therefore, the difference dipole for these mutants cannot be calculated by using derivatives of the absorption spectrum.

The M202HL and M202HL/M160LH mutants belong to a third classification of Stark line shapes. In these mutants, the absorption band is very broad, so a second derivative of the absorption spectrum cannot be reliably obtained. However, it is clear from position of the absorption maxima and Stark minima (Table 1) that these mutants also have an extremely red-shifted Stark spectrum, so $|\Delta\mu|$ cannot be reliably obtained for these mutants by using the derivatives of the absorption spectrum.

To analyze the Stark spectra further, it is useful to compare the positions of the minima of the 2ω Stark spectra with the maxima of the 4ω Stark spectra (see Table 1). Surprisingly, even for mutants in which the 2ω Stark spectrum minimum is significantly shifted from the absorption maximum, the minimum of the 2ω Stark spectrum is at a similar position to the maximum of the 4ω Stark spectrum. Comparison of the second derivative of the 2ω Stark spectrum with the 4ω Stark line shape (Figure 7, bottom panels) further emphasizes this observation. For wild type (lower left panel), the 4ω Stark spectrum is shifted to higher energy relative to the second derivative of the 2ω Stark spectrum and exhibits less structure, so the line shapes are not identical. For L131LH (middle panel), the line shape of the 4ω Stark spectrum matches the line shape of the second derivative of the 2ω Stark spectrum quite well. Finally, for M160LH (right panel), the second derivative of the 2ω Stark spectrum resembles the 4ω Stark spectrum. In all other mutants, including M202HL and M202HL/M160LH, the second derivative of the 2ω Stark spectrum also was found to match the 4ω Stark spectrum.

To compare the magnitude of the Stark effect in all the mutants, we obtain a ratio of the second derivative of the 2ω Stark spectrum to the 4ω Stark spectrum (Table 2). For those mutants in which the second derivative of the absorption matches the Stark line shape, we would expect to obtain the same $|\Delta\mu|$ from this analysis as from the analysis using the second derivative of the absorption spectrum and the 2ω Stark spectrum. Estimated values of $|\Delta\mu|$ based on this approach (eq 3) for these mutants are reported in Table 2. The value of $|\Delta\mu|$ obtained for wild type is 7.5 D, while those obtained for the mutants with Stark line shapes similar to wild type were approximately 10 D. In all cases, the $|\Delta\mu|$ obtained from this method is larger than from the conventional comparison of the second derivative of the absorption to the 2ω Stark data. There are several possible explanations for this difference. First, our model is limited because it considers $\Delta\mu$ to be the only significant contribution to the Stark spectra and does not consider any other contributions, such as the difference polarizability $\Delta\alpha$. Second, the underlying assumptions of the Liptay analysis may not be appropriate for this system, even if the CT state energies are relatively distant. Third, it is possible that the absorption feature that gives rise to the observed Stark spectrum on the low-energy side is buried under an absorption feature whose Stark is much smaller. Using the value of $|\Delta\mu|$ obtained from the ratio of the second derivative of the 2ω Stark spectrum to the observed 4ω Stark spectrum, we can work backward to obtain the putative absorption of such an underlying band. In effect, this uses the Stark spectrum to explore a possible deconvolution of the absorption band. Application of this procedure produces a band on the low-energy side that is much too large to be consistent with the observed absorption, indicating that this mechanism is not operative.

In the following, we will use the ratio of the second derivative of the 2ω Stark effect to the 4ω Stark effect to obtain a better estimate of the comparative magnitudes of the Stark effects in all the different mutants, but we emphasize that these values of $|\Delta\mu|$ are model-dependent. The ratios of the second derivative of the 2ω Stark to the 4ω Stark are given in Table 2. As can be seen from this analysis, there are three groupings in the magnitude of the Stark effect that correspond to the three types of line shapes

described above. First, the M202HL and M202HL/M160 mutants have very large Stark effects with a ratio of ~5000, with the magnitude of the ratio for the double mutant being slightly larger. The second group, which has a smaller ratio (~2500) than the first group, includes M160LH, L173HL, M202HL/L131LH, and L168HG. Finally, the smallest ratios (~1400) are found in the mutants that appear to have Stark effects most similar to wild type: M197FH, L168HF, L168HF/M197FH, L131LH, and L131LH/M160LH/M197FH.

DISCUSSION

Overall Trends. Qualitatively, many of the mutants have absorption and Stark spectra that are significantly different from those of wild type. Both the heterodimer mutants and those that affect hydrogen bonding to the keto carbonyl groups appear to have specific effects on the electrooptic properties of the dimer. Formation of a heterodimer with a BPhe on the M-side results in the largest change relative to wild type, while formation of the L-side heterodimer results in a smaller change in the spectra. Likewise, formation of a hydrogen bond at the keto carbonyl group on the M-side results in changes to the absorption and Stark spectra that are smaller than the M-side heterodimer mutation, while the symmetry-related mutant on the L-side has spectral features that are about the same as those of wild type. Combinations of the heterodimer and keto carbonyl mutations either result in further perturbation from that of wild type (e.g., M202HL/M160LH) or have compensating effects leading to spectra that are more similar to wild type (e.g., M202HL/L131LH). The characteristic changes of both the absorption and Stark spectra can be attributed to the electron-withdrawing effects of the perturbations associated with the mutation and the resulting shifts in the energies of intradimer CT states. A qualitative model for both the absorption and Stark spectra of these mutants and an overall description of the dimer electronic structure deduced from this information will be described below. On the other hand, mutations that change the hydrogen bonds to acetyl carbonyl groups can have little effect on the spectra (e.g., M197FH), can change the position of the absorption spectrum but not the magnitude or line shape of the Stark spectrum (e.g., L168HF), or may alter both the absorption and Stark spectra (e.g., L168HG). These mutants cannot be described by the same model as the one we propose for the keto carbonyl and heterodimer mutants. Possible reasons for the apparent differences in the perturbation of the keto and acetyl carbonyl groups by mutations that affect hydrogen bonds will be discussed below.

Absorption Spectra. The lowest energy absorption bands of the heterodimers and heterodimer/hydrogen-bond mutants have been discussed previously in the context of a molecular exciton state mixing with a single broad CT state (*26*). The two broad features of the dimer band of the M202HL heterodimer could be modeled by assuming an intermediate electronic coupling strength between the two states. A shift in the relative energies of the two states, holding the electronic coupling approximately constant, was shown to alter the relative intensities and bandwidths of the absorption features. For example, when the exciton state is located in the center of the CT band, the resulting absorption band consists of two broad, symmetric bands. Shifting the CT band to higher energy relative to the molecular exciton state causes a narrowing and increase in intensity of the lower-energy band, while the higher-energy band broadens and its intensity decreases.

This model can be used qualitatively to extract information on the location of the CT states for all the mutants reported in this paper. The striking similarity in the absorption line shape of M160LH, L173HL, and M202HL/L131LH suggests that a CT state is located on the high-energy side of the exciton state since the lower-energy feature is narrower and more prominent than the higher-energy band. This type of placement was used to model the absorption line shape of the M202HL/L131LH mutant in some detail (*26*). In wild type and other homodimer mutants, the lower-energy feature is completely dominant, giving the appearance of a narrower absorption band than that of the M160LH mutant. This line shape can be attributed to a CT state that has shifted to higher energy with respect to the exciton state. We stress that this placement of states is qualitative for the homodimers because the model in ref *26* only considers mixing with a single CT state. This is likely appropriate for a quantitative analysis of the heterodimer absorption spectra but not for the homodimers.

Stark Spectroscopy. The conventional analysis of 2ω Stark effect spectra due to Liptay treats the effects of $\Delta\mu$, $\Delta\alpha$, and the oscillator strength as contributing second, first, and zeroth derivatives of the absorption line shape, respectively, to the Stark line shape (eq 1). Typically, the Liptay-type analysis of Stark spectra works well for a transition that involves one ground state and one excited state or instances in which other excited states are sufficiently far away in energy. This includes, for example, monomeric BChl and BPhe both isolated and in the RC [interesting deviations are found in the higher-order Stark spectrum of B_L, discussed in detail elsewhere (*37*)]. The Liptay model also appears sufficient to account for the 2ω Stark spectrum of the dimer band of wild-type RCs and other RCs with similar line shapes. The Stark effect for the special pair in wild-type reaction centers is substantially larger than for BChl, and this has been attributed to a relatively large $\Delta\mu$ associated with the mixing of intradimer CT states with the exciton state (*23*). A more detailed Liptay analysis at very low temperatures showed that there is also a significant first-derivative component to the Stark spectrum, and this was interpreted as indicating a large difference polarizability for the special pair (*35*).

Significant deviations from the expected Liptay line shape have been predicted when the observed transition is significantly coupled to a third (or more) state (*38*, *39*). This situation can lead to variation of the electrooptic parameters across the band. Much of the data presented here also indicates that simple Liptay-type derivative analysis may be inadequate to account for all aspects of the Stark spectra for the dimer. In those RCs that have absorption maxima and 2ω Stark minima at approximately the same position, the second derivative of the absorption dominates the line shape and therefore $\Delta\mu$ would be predicted to be the dominant factor in the Stark line shape. With this assumption, one would expect to obtain about the same $|\Delta\mu|$ from the conventional Stark analysis (eq 2) and the higher-order Stark analysis (eq 3). However, the results of these analyses are systematically different: the conventional analysis gives $|\Delta\mu|$ from 6 to 7 D, while the comparison of the 4ω Stark

spectrum with the second derivative of the 2ω Stark spectrum gives $|\Delta\mu| \approx 10$ D (Table 2). The shortcomings of the analysis are far more apparent for those mutants in which the 2ω Stark line shape is substantially shifted to lower energy compared with the second derivative of the absorption (Figure 7). *No* combination of zeroth, first, and second derivative line shapes of a single band can be used to fit the 2ω Stark spectra for these mutants (e.g., M160LH). Those mutants that have the most significant deviations from the Liptay model are those that are also predicted to have a CT state closer to the exciton state on the basis of the model for the absorption spectra. We therefore attribute this deviation from the Liptay model as an indication of a more significant mixing of the CT state(s) with the exciton state.

Electronic Asymmetry. There has been much discussion on the role of the internal CT states of the dimer and their influence on the asymmetry of the special pair electronic states (*22*−*24*). These intradimer CT states cannot be degenerate in wild type as the excited state breaks the local C_2 symmetry as discussed in the introduction. However, the energy ordering and difference in energy of the two states are not obvious. Calculations suggest that the $P_L^+P_M^-$ state is lower in energy and that the separation between the two intradimer CT states is on the order of 1000 cm^{-1} in wild type (*24*, *40*). In the following, we attempt to correlate the expected shift of CT state energies caused by changes in hydrogen bonding and/or the formation of a heterodimer with the observed changes in the absorption spectra and the magnitudes and line shapes of the Stark spectra.

The mutations that add hydrogen bonds to the keto carbonyl groups cause comparable increases in the oxidation potential of P, +65 and +85 mV relative to wild type for M160LH and L131LH, respectively (*16*). The keto carbonyl stretching frequencies also shift by about the same amount in these mutants (*18*), suggesting that the perturbations are approximately equivalent on the opposite ends of the special pair (cf. lower part of Figure 1). These mutations should have different effects on the asymmetry of the dimer because adding a hydrogen bond to the L-side stabilizes the $P_L^-P_M^+$ state and destabilizes the $P_L^+P_M^-$ state, and the converse is expected when a hydrogen bond is added to the M-side. As can be seen in Figure 3, the absorption and Stark spectra of these two mutants are vastly different, implying that lowering the $P_L^+P_M^-$ state and raising the $P_L^-P_M^+$ state has a significant effect on the dimer band, while lowering the $P_L^-P_M^+$ state and raising the $P_L^+P_M^-$ state has little effect on the dimer band.

Figure 8 presents a schematic diagram of the changes in state energies that can be used to systematically model the observed effects. The starting point of this model requires that the $P_L^+P_M^-$ state is located closer energy to the exciton state than $P_L^-P_M^+$ in wild type. As will be seen in the following, only this assignment leads to a self-consistent analysis of all of the data. Upon addition of a hydrogen bond to P_M, the $P_L^+P_M^-$ state is lowered and the $P_L^-P_M^+$ state is raised, thus increasing the asymmetry of the excited state. The increased separation of the two CT states, with the $P_L^+P_M^-$ state moving closer to the exciton state, combine to account for the increased Stark effect as well as the observed change in the absorption and Stark line shapes. For L131LH, the excited state of the dimer retains about the same characteristics of asymmetry as that of wild type. Since one

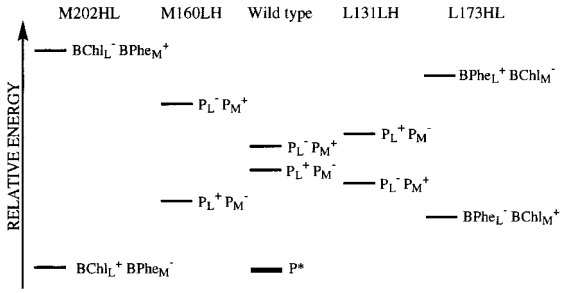

FIGURE 8: Diagrammatic representation of the relative energies of the CT states in reaction center mutants based on the qualitative analysis of the results. The pure exciton state P* is assumed to remain the same for all the mutants, while the charge-transfer state energies are perturbed. The charge-transfer states are represented as narrow lines; however, these represent the maximum of a broad CT band (*26*).

would predict stabilization of the $P_L^-P_M^+$ state and destabilization of the $P_L^+P_M^-$ state in this mutant, the energy ordering of the CT states *must be reversed* in order for the special pair in this mutant to maintain the same amount of asymmetry as wild type. This leads to the conclusion that the L131LH mutant has approximately the same amount of asymmetry as wild type *but the direction is different*.

The observed line shapes in the heterodimer mutants can also be understood with the model shown in Figure 8. Replacement of the BChl P_M by a BPhe, which is easier to reduce than BChl, lowers the energy of the $P_L^+P_M^-$ (now $BChl_L^+BPhe_M^-$) state and increases the energy of the $P_L^-P_M^+$ (now $BChl_L^-BPhe_M^+$) state. The shifts in the energies of the states are larger for the mutation to BPhe than just the addition of a hydrogen bond, causing a greater asymmetry in the dimer. Therefore, the absorption spectrum is very broad and the Stark effect is large. The L173HL mutation moves the other CT state, $BPhe_L^-BChl_M^+$, closer to the exciton state and shifts the $BPhe_L^+BChl_M^-$ state higher in energy. However, because of the starting position of these states in wild type, the excited state of the dimer in the L173LH mutant is less asymmetric than in the M202HL mutant; it is comparable (but reversed in sign) to the asymmetry found in the M160LH mutant. In the M202HL double mutants, the addition of hydrogen bonds further alters the position of the CT states. The addition of a hydrogen bond to the M side of the dimer increases the asymmetry; in fact, in this mutant a more detailed analysis of the absorption spectrum suggests that the center of the CT state is well below the energy of the exciton state (*26*). However, the magnitude of the Stark effect is not much greater than the Stark effect in M202HL. Addition of a hydrogen bond to the L-side of the dimer decreases the asymmetry of the dimer, and the $BChl_L^+BPhe_M^-$ state is increased in energy relative to that of the exciton state. This results in absorption and Stark spectra that are similar to those of the M160LH and L173LH mutants.

Another way to visualize the perturbations on the electronic structure of the excited state is presented in Figure 9. The dimer is considered to be an extended π-system from the keto carbonyl on the L side to the keto carbonyl on the M side (see lower part of Figure 1) (*26*). In wild type, there is a small asymmetry in the excited state, characterized by more electron density on the M-side of the dimer. Addition of a hydrogen bond to the keto carbonyl on the M-side of the dimer causes the electron density to be pulled toward

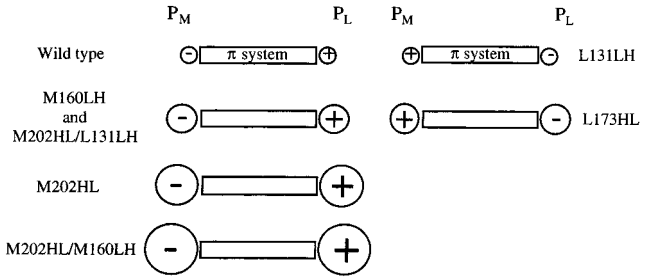

FIGURE 9: Schematic representation of the electron density on the L versus M side of the dimer in the different reaction centers. The rectangle represents the extended π system of the dimer; the circles represent the relative amount of electronic asymmetry on each side of the dimer π system. At the top left, wild type is shown to have a small amount of electronic asymmetry, with more electron density on the M-side. Mutants on the left are found to be asymmetric in the same direction as wild type, but with increasing magnitude of the perturbation indicated by larger circles. Mutants on the right are found to be asymmetric in the opposite direction as wild type, but with increasing magnitude of the perturbation indicated by larger circles. The LH131 dimer has about the same magnitude of asymmetry as wild type, and this asymmetry is increased in the L173HL mutant.

the M-side of the dimer and therefore increases the asymmetry. Replacement of $BChl_M$ with a BPhe is a more severe change than the addition of a hydrogen bond and leads to a greater electron density on the M side. Some of the electron density on the M-side of the heterodimer can be pulled back toward the L side by adding a hydrogen bond to the L-side keto carbonyl group, as demonstrated by the decreased magnitude of the Stark effect (compared to heterodimer) in the M202HL/L131LH mutant. Likewise, adding a hydrogen bond to the L side keto carbonyl of the homodimer causes a shift in the electron density toward the opposite side; however, the magnitude of asymmetry remains about the same as wild type. Finally, when $BChl_L$ is replaced by a BPhe, the asymmetry is also reversed and the magnitude of the asymmetry is less than for the M-side heterodimer. Described this way, the special pair electronic structure is much like a donor−acceptor ("push−pull") substituted polyene system in which the donor and acceptors can be varied to modulate the electrooptic properties of the molecule (*41*).

Mutations near the Acetyl Carbonyls. Most of the mutants in which hydrogen bonds to the acetyl groups are changed (M197FH, L168HF, L168HF/M197FH) have Stark effects that are similar in line shape and magnitude to the wild-type spectra. These results are surprising as modifications of the hydrogen bonds at the acetyl groups have been shown to significantly perturb the P^+/P oxidation potential (*16*), and the large changes in the carbonyl stretching modes suggest that the added or removed hydrogen bonds are relatively strong (*18*). In all these mutants, one would expect the electron density to become greater on the M side of the dimer. In fact, if the magnitude of the change in oxidation potential can be used as a guide, one would expect to see larger changes in these mutants than in the M160LH mutant.

The relative insensitivity of the absorption and Stark spectra to mutations in these positions could be due, in part, to the fact that hydrogen-bond perturbations are located too close to the center of the π-system and therefore may be ineffective in pulling the electron density from one side of the dimer to the other. However, the data from the L168HG mutant, which has a large Stark effect much like that of the M160LH mutant, suggest that this simple interpretation may not be correct. In particular, the model presented here requires that all cases being compared share the same π system. The acetyl groups are conjugated to the π system, and it is likely that removal of the hydrogen bond to the acetyl groups changes the conformation of the acetyl group. This is reflected in the blue-shifted absorption spectra of these mutants (*42*, *24*). It is also likely that different mutations at this position (Phe and Gly) lead to different conformations of the acetyl group, since the maxima of the dimer absorption bands are not the same. The Stark effect should also depend significantly on the structure of the π-system, so it is reasonable that the differences between L168HF, which has a Stark effect like that of wild type, and L168HG mutant, which has a Stark effect more similar to that of M160LH, arise from different conformations of the acetyl group in the two mutants. The L168HG mutant is similar to the L168HF mutant in all other respects, as it has been confirmed that the hydrogen bond to the P_L acetyl group is removed and the redox potentials obtained for the two mutants are approximately the same (*43*).

Different Meanings of Asymmetry in ^1P, P^+, and ^3P. The amount of asymmetry in the oxidized ground state of the dimer P^+ has been evaluated by ENDOR spectroscopy for many mutants (*44*, *45*). As expected, the heterodimers are highly asymmetric with the unpaired electron (hole) almost completely localized on the more easily oxidized BChl pigment. However, there appears to be less asymmetry in the L173HL mutant than in the M202HL mutant (*44*), which qualitatively agrees with the observations of the excited-state asymmetry described here. For the keto carbonyl hydrogen-bond mutants, the M160LH mutant has been shown to be more asymmetric than wild type, while the L131LH mutant was found to be more symmetric than wild type (*45*). This is not entirely consistent with excited-state observations: the M160LH mutant is more asymmetric than wild type, but the L131LH mutant appears to retain about the same asymmetry as wild type. Likewise, while the L131LH/M202HL mutant shows less asymmetry than the M202HL mutant from the evaluation of the Stark spectra, ENDOR spectroscopy suggests that the hole is completely localized on the BChl molecule. Results from ENDOR experiments on the acetyl carbonyl hydrogen-bond mutants also show that P^+ is more symmetric in the L168HF mutant, while the M197FH mutant has about the same amount of asymmetry as wild type, and it was also suggested that the conformation of the acetyl group is an important factor in understanding the results (*45*). For both of these mutants, the asymmetry in the excited state appears to be about the same as in wild type.

The triplet state of P has also been examined in some of the mutants by low-temperature (1.5 K) absorption-detected magnetic resonance (*46*, *47*). For the L131LH and M160LH mutants, the electronic structure of the triplet state was found to be the same as that of wild type (*47*). For the heterodimers, the data suggest that the triplet state is largely localized on the BChl half of the dimer, although the L- and M-side heterodimers are not equivalent (*46*). Therefore, it appears that the observations from experiments on P^+ and ^3P can be related to those obtained for the excited state in the heterodimers but not for the hydrogen-bond perturbations.

Although earlier studies demonstrate that the electronic asymmetry of the dimer can be perturbed by hydrogen bonds and heterodimer formation, they do not address the functionally important question of how the electronic characteristics of ^{1}P are perturbed. The characteristics of ^{1}P are, of course, of particular interest because this could have a significant effect on both the rate and the quantum yield of electron transfer. Since the asymmetry of the dimer should affect the overlap of the orbitals involved in electron transfer between the donor and acceptor, one would expect to see a different effect when the mutations occur on the opposite side. Therefore, if coupling is maximized with more electron density on the M-side of the dimer (the situation in wild type), one would expect the rates of the L-side mutations to be slower than the corresponding M-side mutations. Additionally, it has been argued that the increase in CT character in ^{1}P leads to an increase in the nonradiative decay rate, reducing the quantum yield of charge separation in the heterodimer mutant (*12*).

These expectations are borne out in this series of mutants. The primary charge separation rates are slower in both the L-side heterodimer and L-side keto hydrogen bond mutants rates than in the corresponding M-side mutants. For the heterodimer mutant, the electron-transfer rate to H_L is reported to be about $(80\ ps)^{-1}$ in M202HL, while it is at least 2 times slower in the L-side heterodimer (*12*). Likewise, the electron-transfer rate to H_L is about 2 times slower in the L-side hydrogen-bond mutant as in the M-side hydrogen-bond mutant (*12*). The quantum yields of both the nonradiative decay to the ground state and electron transfer to form $P^+H_L^-$ depend on the relative rates of these two processes. So although the excited states in L-side mutants have less CT character than in the corresponding M-side mutants, the quantum yields of electron transfer are similar (*12*, *13*) because of the slower rate of electron transfer to H_L.

ACKNOWLEDGMENT

We are very grateful to Professors Allen, Williams, and Woodbury at Arizona State University, who made strains available.

REFERENCES

1. Kirmaier, C., and Holten, D. (1987) *Photosynth. Res. 13*, 225−260.
2. Boxer, S. G., Goldstein, R. A., Lockhart, D. J., Middendorf, T. R., and Takiff, L. J. (1989) *J. Phys. Chem. 93*, 8280−8294.
3. Rautter, J., Lendzian, F., Lubitz, W., Wang, S., and Allen, J. P. (1994) *Biochemistry 33*, 12077−12084.
4. Lendzian, F., Huber, M., Issacson, R. A., Endeward, B., Plato, M., Bonigk, B., Mobius, K., Lubitz, W., and Feher, G. (1993) *Biochim. Biophys. Acta 1183*, 139−160.
5. Breton, J., Nabedryk, E., and Parson, W. W. (1992) *Biochemistry 31*, 7503−7510.
6. Reimer, J. R., and Hush, N. S. (1995) *Chem. Phys. 197*, 323−334.
7. Norris, J. R., Budil, D. E., Gast, P., Chang, C.-H., El-Kabbani, O., and Schiffer, M. (1989) *Proc. Natl. Acad. Sci. U.S.A. 86*, 4335−4339.
8. Takiff, L., and Boxer, S. G. (1988) *Biochim. Biophys. Acta 932*, 325−334.
9. Kirmaier, C., Holten, D., Bylina, E. J., and Youvan, D. C. (1988) *Proc. Natl. Acad. Sci. U.S.A. 85*, 7562−7566.
10. Hammes, S. L., Mazzola, L., Boxer, S. G., Gaul, D. F., and Schenck, C. C. (1990) *Proc. Natl. Acad. Sci. U.S.A. 87*, 5682−5686.
11. DiMagno, T. J., Bylina, E. J., Angerhofer, A., Youvan, D. C., and Norris, J. (1990) *Biochemistry 29*, 899−907.
12. Laporte, L., McDowell, L. M., Kirmaier, C., Schenck, C. C., and Holten, D. (1993) *Chem. Phys. 176*, 615−629.
13. Williams, J. C., Alden, R. G., Murchison, H. A., Peloquin, J. M., Woodbury, N. W., and Allen, J. P. (1992) *Biochemistry 31*, 11029−11037.
14. Stocker, J. W., Taguchi, A. K. W., Murchison, H. A., Woodbury, N. W., and Boxer, S. G. (1992) *Biochemistry 31*, 10356−10362.
15. Murchison, H. A., Alden, R. G., Allen, J. P., Peloquin, J. M., Taguchi, A. K. W., Woodbury, N. W., and Williams, J. C. (1993) *Biochemistry 32*, 3498−3505.
16. Lin, X., Murchison, H. A., Nagarajan, V., Parson, W. W., Allen, J. P., and Williams, J. C. (1994) *Proc. Natl. Acad. Sci. U.S.A. 91*, 10265−10269.
17. Nabedryk, E., Allen, J. P., Taguchi, A. K. W., Williams, J. C., Woodbury, N. W., and Breton, J. (1993) *Biochemistry 32*, 13879−13885.
18. Mattioli, T. A., Williams, J. C., Allen, J. P., and Robert, B. (1994) *Biochemistry 33*, 1636−1643.
19. Mattioli, T. A., Lin, X., Allen, J. P., and Williams, J. C. (1995) *Biochemistry 34*, 6142−6152.
20. Ivancich, A., Artz, K., Williams, J. C., Allen, J. P., and Mattioli, T. A. (1998) *Biochemistry 37*, 11812−11820.
21. Lathrop, E. J. P., and Friesner, R. A. (1994) *J. Phys. Chem. 98*, 3056−3066.
22. Boxer, S. G. (1990) *Annu. Rev. Biophys. Biophys. Chem. 19*, 267−299.
23. Lockhart, D. J., and Boxer, S. G. (1988) *Proc. Natl. Acad. Sci. U.S.A. 85*, 107−111.
24. Parson, W. W., and Warshel, A. (1987) *J. Am. Chem. Soc. 109*, 6152−6163.
25. Thompson, M. A., Zerner, M. C., and Fajer, J. (1991) *J. Phys. Chem. 95*, 5693−5700.
26. Zhou, H., and Boxer, S. G. (1997) *J. Phys. Chem. 29*, 5759−5766.
27. Fajer, J., Brune, D. C., Davis, M. S., Forman, A., and Spaulding, L. D. (1975) *Proc. Natl. Acad. Sci. U.S.A. 72*, 4956−4960.
28. Goldsmith, J. O., King, B., and Boxer, S. G. (1996) *Biochemsitry 35*, 2421−2428.
29. Goldsmith, J. O., and Boxer, S. G. (1996) *Biochim. Biophys. Acta 1276*, 171−175.
30. Paddock, M. L., Rongey, S. H., Abresch, E. C., Feher, G., and Okamura, M. Y. (1988) *Photosynth. Res. 17*, 75−91.
31. Boxer, S. G. (1993) in *The Photosynthetic Reaction Center* (Deisenhofer, J., and Norris, J. R., Eds.) pp 179−220, Academic Press, San Diego, CA.
32. Bublitz, G. U., and Boxer, S. G. (1997) *Annu. Rev. Phys. Chem. 48*, 213−242.
33. Liptay, W. (1974) in *Excited States* (Lim, E. C., Ed.) pp 129−229, Academic Press, New York.
34. Mathies, R. A. (1974) Ph.D. Thesis, Cornell University, Ithaca, NY.
35. Middendorf, T. R., Mazzola, L. T., Lao, K., Steffen, M., and Boxer, S. G. (1993) *Biochim. Biophys. Acta 1143*, 223−234.
36. Lao, K., Moore, L. J., Zhou, H., and Boxer, S. G. (1995) *J. Phys. Chem. 99*, 496−500.
37. Zhou, H., and Boxer, S. G. (1998) *J. Phys. Chem. 102*, 9139−9147 and 9148−9160.
38. Wortmann, R., Elich, E., and Liptay, W. (1988) *Chem. Phys. 124*, 395−409.
39. Reimers, J. R., and Hush, N. S. (1991) in *Mixed Valence Systems: Applications in Chemistry, Physics and Biology* (Prassides, K., Ed.) pp 29−50, Kluwer Academic Publishing, Dordrecht, The Netherlands.
40. Scherer, P. O. J., and Fischer, S. F. (1991) in *Chlorophylls* (Scheer, H., Ed.) pp 1079−1093, CRC Press, Boca Raton, FL.

41. Bublitz, G. U., Ortiz, R., Marder, S. R., and Boxer, S. G. (1997) *J. Am. Chem. Soc. 119*, 3365−3376.
42. Plato, M., Lendzian, F., Lubitz, W., and Möbius, K. (1992) in *The Photosynthetic Bacterial Reaction Center II: Structure, Spectroscopy and Dynamics* (Breton, J., and Verméglio, A., Eds.) pp 109−118, Plenum Press, New York.
43. Moore, L. J. (1998) Ph.D. Thesis, Stanford University, Stanford, CA.
44. Huber, M., Isaccson, R. A., Aberch, E. C., Gaul, D., Schenck, C. C., and Feher, G. (1996) *Biochim. Biophys. Acta 1273*, 108−128.
45. Rautter, J., Lendzian, F., Schulz, C., Fetsch, A., Kuhn, M., Lin, X., Williams, J. C., Allen, J. P., and Lubitz, W. (1995) *Biochemistry 34*, 8130−8143.
46. Vrieze, J., Schenck, C. C., and Hoff, A. J. (1996) *Biochim. Biophys. Acta 1276*, 229−238.
47. Vrieze, J., Williams, J. C., Allen, J. P., and Hoff, A. J. (1996) *Biochim. Biophys. Acta 1276*, 221−228.
48. Deisenhofer, J., Epp, O., Sinning, I., and Michel, H. (1995) *J. Mol. Biol. 246*, 429−457.

BI990892J